Integral floating display systems for augmented reality

Jisoo Hong,[1] Sung-Wook Min,[2,*] and Byoungho Lee[1]

[1]School of Electrical Engineering, Seoul National University, Gwanak-Gu Gwanakro 1, Seoul 151-744, South Korea

[2]Department of Information Display, Kyung Hee University, 1 Hoeki-Dong Dongdaemoon-Gu, Seoul 130-701, South Korea

*Corresponding author: mins@khu.ac.kr

Received 7 February 2012; revised 12 April 2012; accepted 1 May 2012;
posted 2 May 2012 (Doc. ID 162689); published 18 June 2012

Novel integral floating three-dimensional (3D) display methods are proposed for implementing an augmented reality (AR) system. The 3D display for AR requires a long-range focus depth and a see-though property. A system that adopts a concave lens instead of a convex lens is proposed for realizing the integral floating system with a long working distance using a reduced pixel pitch of the elemental image. An investigation that reveals that the location of the central depth plane is restricted by the pixel pitch of the display device is presented. An optical see-through system using a convex half mirror is also proposed for providing 3D images with a proper accommodation response. The concepts of the proposed methods are explained and the validity of system is proved by the experimental results.

OCIS codes: 110.2990, 100.6890.

1. Introduction

With developments in computer science, AR has recently become an actively researched field [1]. The purpose of AR is to create an experience in which additional information is mixed with the five human senses. The display device used in AR systems should have the capability to overlay an artificial image onto a real world scene in order to present an AR to the human visual sense. A number of display devices have been proposed for providing AR functionality for human vision. Head-mounted display (HMD) has been investigated since the early stages of AR research and it can be categorized into video see-through and optical see-through types [2]. Optical see-through HMD has a relatively shorter history than the video see-through type and some unresolved issues related to the optical see-through HMD still remain. One of these is the accommodation mismatch between the virtual image and the real-world scene that arises because the gap between the real-world scene and the virtual image is usually so large that the human visual system (HVS) cannot accommodate them both. The other issue is the demand to display 3D images of the overlaid virtual information. Liu *et al.* proposed an HMD system that adopts a liquid lens for dynamically changing the optical distance of the virtual image [3]. Though their report showed that the accommodation response was successfully addressed, their system cannot display 3D images. The recent super multi-view (SMV) theory provides a way to display 3D images with an accommodation response corresponding to the intended distance. Takaki *et al.* presented an optical see-through system that satisfies the SMV condition of providing a distant 3D image with a precise accommodation response [4]. Though their system successfully provides 3D images with proper accommodation cues, the implementation of SMV has an inherent difficulty in that it demands an excessive number of rays per lateral 3D image pixel. As seen from many reports related to SMV, the SMV system is usually implemented in the form of a highly complicated system with a large volume in order to make use of time or spatial multiplexing [5]. Hence, the SMV feature is not adequate for HMD adoption. The implementation of HMD providing 3D images of

1559-128X/12/184201-09$15.00/0

an appropriate accommodation cue still remains to be investigated.

Integral imaging (InIm), which was first proposed by Lippmann in 1908, is a 3D display method that provides full-parallax autosteroscopic images with relatively simple optics [6,7]. There are two types of implementation—called the real/virtual mode and the focused mode, respectively—according to the gap between the elemental image and the lenslet array. In order to emphasize the advantageous features of each method, they are sometimes also called "resolution-priority InIm" and "depth-priority InIm" [8]. In general, the real/virtual mode implementation of InIm is thought to be able to express a 3D image around the central depth plane, where the focal planes of each lenslet of the lenslet array are superposed, regardless of location [9]. One might expect that the optical see-through HMD without issues described above can be realized using the virtual mode InIm if the longitudinal range of the 3D image is not too large. However, general observations from experiments related to the real/virtual mode InIm show that the central depth plane location is restricted to a certain range, which means that a displayed 3D image cannot go farther than a certain distance.

In this article, we propose an integral floating system with a concave floating lens that can be applied for HMD with a 3D image satisfying an accommodation response based on the principle of the virtual mode InIm. As investigated in Section 2, the pixel pitch of a display panel that is adopted for the system is mainly related to the upper bound of the distance of the central depth plane from the lenslet array when the system is the virtual mode InIm. The use of a concave floating lens effectively reduces the pixel pitch of the display panel and extends the expressible range of the 3D image. We analyze the characteristics of the proposed system and verify them by experimental results. To impose a see-through characteristic on the proposed scheme, we present a system adopting a convex half mirror. The AR system can be successfully implemented using the proposed convex half mirror, which has the same optical property as the concave lens.

2. Limitations in a Long Distance Integral Image

The final goal of this study is to design an integral floating system with a see-through characteristic in the form of HMD for the purpose of AR, as shown in Fig. 1. Instead of a concave mirror, which is equivalent to the convex floating lens of the conventional integral floating system, the proposed scheme adopts a convex mirror as a floating optic. This configuration can be interpreted as an effective InIm system with various parameters changed (see Fig. 2). A detailed explanation will be provided in Section 3. As described before, a significant problem of the HMD-type AR system is that there is usually a large difference between the accommodation cues of the real-world scene and the virtual image. In this section, the limitations in long distance imaging by

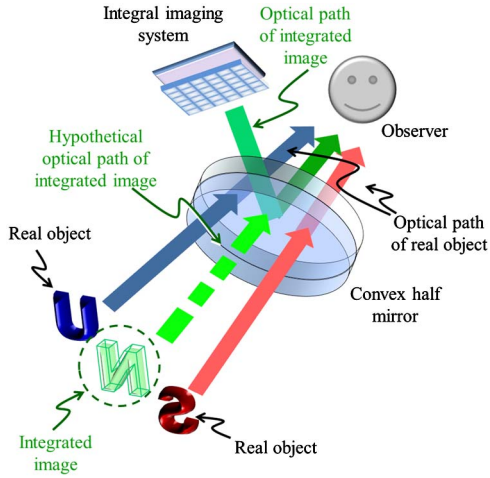

Fig. 1. (Color online) Concept of optical see-through HMD based on an integral floating scheme adopting a convex half mirror. The integrated image is provided to the observer through the optical path specified as the "optical path of integrated image." The integrated image appears as a virtual image behind the convex half mirror; therefore, the perceived optical path is a dashed arrow specified as the "hypothetical optical path of integrated image."

the InIm method and their relationship to the system specifications are investigated in terms of three different constraints: the lateral pixel pitch of the integrated image should satisfy a given angular resolution requirement, Eq. (2); the minimum resolvable depth around the central depth plane should be smaller than the depth discrimination of the HVS, Eq. (8); and the central depth plane should be located inside the available voxels, Eq. (10). The result of this investigation will be used in designing the proposed system to address the appropriate accommodation response from the displayed integrated images corresponding to a given real-world scene.

As discussed in [10], the resolution (or pixel pitch) of the display device used for implementation of the InIm system is a fundamental resource for three important visual quality factors: the lateral resolution,

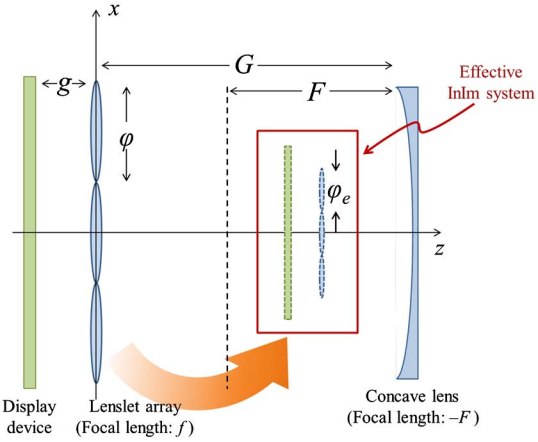

Fig. 2. (Color online) Interpretation of an integral floating scheme adopting a concave lens instead of a convex lens. The entire system can be interpreted as an effective InIm system.

viewing angle, and marginal depth, of a displayed 3D image. In other words, the visual quality of a displayed 3D image is limited by the pixel pitch of the display device adopted for the InIm system. Under a given pixel pitch, it is only possible to balance the quality factors; one quality factor can be enhanced by degrading other factors. The viewing angle of most InIm systems is not large enough, though it is a very critical quality factor. Therefore, a number of techniques have been developed for enhancing the InIm viewing angle with various additional hardware components [11]. Hence, it is very important to define an appropriate lower bound for the viewing angle and strictly design the system accordingly. For simplicity, we define the viewing angle parameter Ω as follows:

$$\Omega = 2\tan^{-1}\left(\frac{\theta}{2}\right), \tag{1}$$

where θ is the viewing angle of the system.

In our discussion, only the virtual mode of the InIm scheme, in which the central depth plane is located behind the lenslet array, is considered. Figure 3 shows the parameters defined for further discussions. To utilize the virtual mode of the InIm system, the lateral pixel pitch of the integrated image, P_I, should be smaller than the pitch of each lenslet of the lenslet array, φ, as described in [10]. However, this point should be revisited because a lateral resolution perceived by an observer is assessed by angular resolution (cycles per degree). A more exact restriction on the lateral resolution can be found by considering human visual acuity. The required lateral resolution of the display device, defined as cycles per degree (or lines per degree), is well established in the conventional two-dimensional (2D) display device. For a given angular resolution requirement, say m lines per degree (lpd), the lateral pixel pitch of the integrated image, P_I, is limited by the inequality

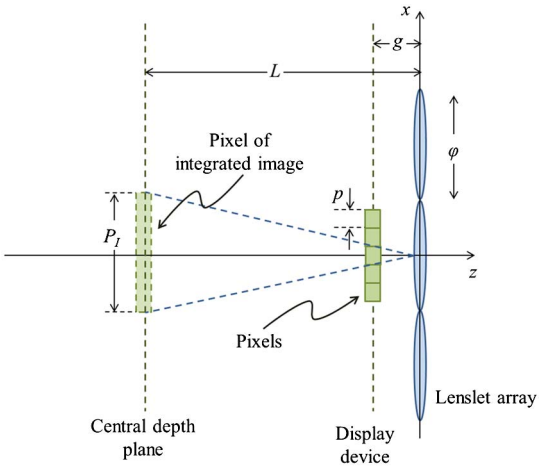

Fig. 3. (Color online) Definition of parameters used for analysis in the virtual mode InIm scheme.

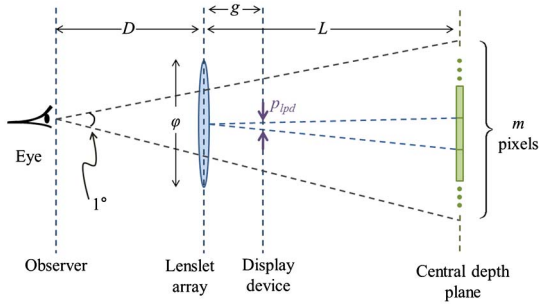

Fig. 4. (Color online) Relationship between lenslet pitch and lateral pixel pitch of the integrated image used for enabling virtual mode InIm. Human visual acuity is also depicted as cycles per degree.

$$P_I < \frac{\pi}{180}\frac{(L+D)}{m}, \tag{2}$$

where D is the distance between the observer and the lenslet array, and L the distance between the central depth plane and the lenslet array, (see Fig. 4); Otherwise, this inequality can be rewritten using the pixel pitch of the display device, p, as follows:

$$\frac{L\Omega}{\varphi}p < \frac{\pi}{180}\frac{(L+D)}{m}, \tag{3}$$

considering that $\Omega = \varphi/g$ and $P_I = pL/g$. Equation (3) can be rewritten by imposing an upper bound on L as follows:

$$L < \frac{D}{\left(\frac{180}{\pi}\frac{mp\Omega}{\varphi} - 1\right)}, \tag{4}$$

and this inequality is valid only when

$$p > \frac{\pi}{180}\frac{\varphi}{m\Omega} = p_{\mathrm{lpd}}, \tag{5}$$

where p_{lpd} is the required pixel pitch subject to a given angular resolution requirement (m lpd) for the case where the observer is located at the position of the lenslet array. The perceived angular resolution increases as the observer goes farther from the lenslet array; therefore, if $p \le p_{\mathrm{lpd}}$, the constraints given by Eq. (2) will always hold; therefore Eq. (4) is meaningless.

Equation (4) shows the upper bound of L has a dependence on φ as well as p. However, a large φ value cannot be freely determined to give proper depth information to the observer. To provide an accurate depth cue to the observer, the images shown to the left and right eyes of an observer should be independent of each other and not cause cross talk in disparity information as shown in Fig. 5. On the basis of Eq. (9) in [12], the size of φ should be limited by an inequality:

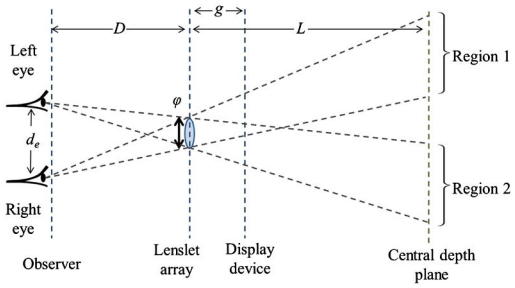

Fig. 5. (Color online) Conditions for avoiding cross talk between the disparity information of left and right eyes. Regions 1 and 2 should be completely separated.

$$\varphi < \frac{L}{L+D} d_e, \tag{6}$$

where d_e is the distance between the eyes of the observer, to avoid the cross talk in the disparity information. From Eq. (6), though the upper bound of φ varies according to the values of L and D, φ cannot be larger than d_e for any case. It is well known that the distance between human eyes is around 65 mm; this means that φ cannot be larger than 65 mm. Hence, the upper bound of L is mainly affected by p under the condition of Eq. (6).

The longitudinal quantization step (or depth resolution) of the system should also be taken into account to assess its performance as a 3D display device. Following a similar analysis shown in [4], the minimum resolvable depth around the central depth plane of the displayed integrated image can be estimated. It can be easily calculated by finding the perceived depth when the left and right eyes of an observer focus on different adjacent pixels on the central depth plane as shown in Fig. 6. Accordingly, the calculated minimum resolvable depths in front of and behind the central depth plane are

$$\delta_f = \frac{P_I(L+D)}{d_e + P_I},$$
$$\delta_b = \frac{P_I(L+D)}{d_e - P_I}, \tag{7}$$

respectively. The system's design is expected to have a longitudinal resolution, determined by Eq. (7),

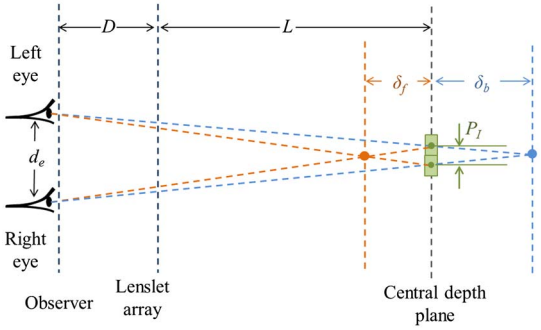

Fig. 6. (Color online) Minimum quantization step of the displayed integrated image around the central depth plane.

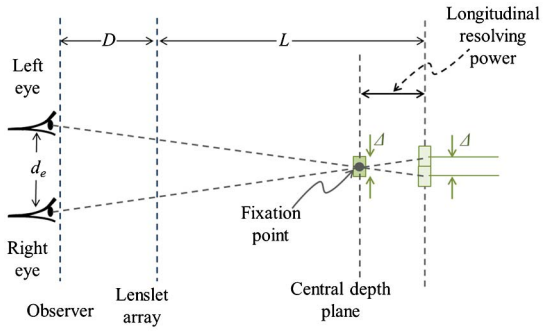

Fig. 7. (Color online) Depth discrimination (or longitudinal resolving power) of the HVS around the central depth plane.

which is higher than the depth discrimination of the HVS. The minimum resolvable longitudinal distance for humans is related to various factors and deducing an accurate expression is difficult. We will consider a relatively loose condition for the longitudinal resolving power of the HVS based on the perceived disparity. As shown in Fig. 7, the longitudinal resolving power around the central depth plane is determined by the range in which the disparity information is confused by the restriction in human visual acuity. Hence, δ_b should be restricted by the inequality

$$\delta_b = \frac{P_I(L+D)}{d_e - P_I} < \frac{\pi}{180} \frac{(L+D)^2}{d_e m}. \tag{8}$$

From this relationship, the upper bound of L can be calculated as follows:

$$L < \frac{1}{2}\left[\left(\frac{\varphi d_e}{p\Omega} - \frac{180}{\pi} d_e m - D\right) + \sqrt{\left(\frac{\varphi d_e}{p\Omega} - \frac{180}{\pi} d_e m - D\right)^2 + \frac{4\varphi d_e D}{p\Omega}}\right]. \tag{9}$$

Of course, the actual upper bound of L should be much smaller than that in Eq. (9) because we used the loose requirement. However, Eq. (9) can be useful for investigating the tendencies of the upper bound of L according to various parameters. Other than the limitation related to human depth discrimination, L is also restricted by a finite range of voxels created by the InIm system. It was determined that the locations of the available voxels, which are determined by points where at least two different rays cross, are limited inside a certain range owing to the finite pixel pitch of the display panel [8]. Such a range is bounded by Ng, where N is the number of pixels per lenslet of the lenslet array, and g is the gap between the lenslet array and the display panel. The voxels exist at the farthest $(L + Ng)$ distance from the lenslet array, meaning that the InIm cannot display a 3D image over this distance. However,

considering the perceived depth resolution determined by Eq. (7), there should be at least one resolvable depth behind the central depth plane because the longitudinal expressible range of InIm is determined around the central depth plane. Hence, to show a 3D image behind the central depth plane, $(L+\delta_b) < (L+Ng)$, i.e.,

$$\delta_b = \frac{P_I(L+D)}{d_e - P_I} < Ng. \tag{10}$$

This limitation can be rewritten as follows:

$$L < \frac{d_e\varphi^3}{p^2\Omega^2 D + p\varphi(\varphi+d_e)\Omega}. \tag{11}$$

Combining Eqs. (4), (9), and (11), the limitation becomes

$$L < \min\left(\frac{1}{2}\left[\left(\frac{\varphi d_e}{p\Omega} - \frac{180}{\pi}d_e m - D\right) + \sqrt{\left(\frac{\varphi d_e}{p\Omega} - \frac{180}{\pi}d_e m - D\right)^2 + \frac{4\varphi d_e D}{p\Omega}}\right], \frac{d_e\varphi^3}{p^2\Omega^2 D + p\varphi(\varphi+d_e)\Omega}, \frac{D}{\left(\frac{180}{\pi}\frac{mp\Omega}{\varphi} - 1\right)}\right). \tag{12}$$

where $\min(A,B,C)$ means the minimum value of A, B, and C.

Figure 8 shows the simulation results demonstrating the way in which the upper bound of L is affected by p, Ω, and m. The angular resolution of the displayed image, m, is a subjective parameter that varies according to the acceptable visual quality decision. The widely accepted standard in the 2D display industry claims that 60 lpd is enough to satisfy human visual acuity [13]. However, it is common to regard a much lower visual quality as acceptable for a 3D display system, considering the present status of display devices. Our group often uses a lenslet array with a pitch of 1 mm for the InIm focal mode for research purposes [14]. From a distance of about 600 mm, which corresponds to about 10 lpd, the display quality is such that simple symbols are recognizable. Considering that our goal is to implement HMD, for calculation, D and Ω are set to 100 mm and 0.2, respectively, and the required φ is assumed to be 2 mm. As shown in Fig. 8(a), the upper bound for 30 lpd and 60 lpd is mostly ruled by depth discrimination, which is explained by Eq. (9). However, the upper bound for 10 lpd is ruled by the existence of voxels when p is smaller than around 18 μm. Considering an angular resolution of 10 lpd, we can see that the 3D image can be displayed at 1000 mm behind the lenslet array for $p < 18$ μm. However, an angular resolution of 30 lpd requires p to be smaller than 6 μm, which nearly approaches the current best spatial light modulator based on liquid crystals [15] and 60 lpd requires a much smaller pixel pitch, even for displaying 3D images at a distance of 1000 mm. Hence, it can be said that displaying 3D images of 60 lpd at farther than 1000 mm still needs further development. Figure 8(b) shows the dependence of the upper bound on the viewing angle of the system. As expected, the viewing angle has a tradeoff relationship with the upper bound of the central depth plane. The viewing angle used for Fig. 8(a) corresponds to approximately 11.4°. Hence, a greatly reduced pixel pitch is required for enlarging the viewing angle.

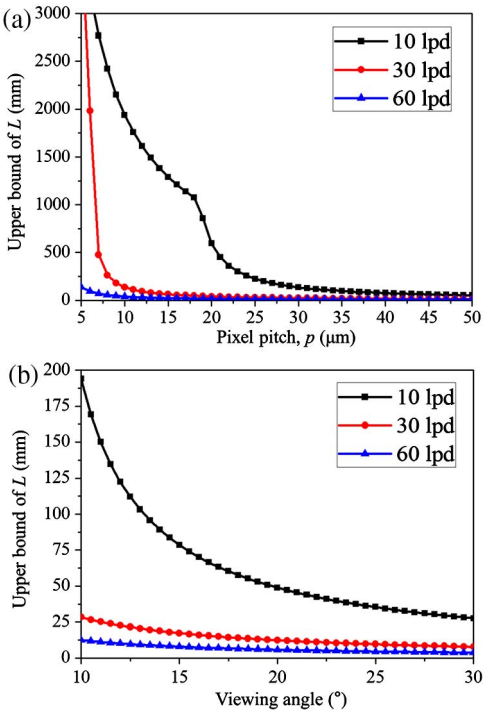

Fig. 8. (Color online) Results of a numerical simulation showing the dependence of the upper bound of L on p, φ, and m. (a) Upper bound according to p and m, (b) upper bound according to θ and m.

3. Integral Floating Display Using a Convex Half Mirror

Integral floating display is a 3D display technique that combines an InIm scheme and a floating technique. Previous research has demonstrated that an integral floating system can show more advantageous features than an InIm system, owing to an additional convex lens [16,17]. The additional convex lens results in a wider viewing angle and a larger depth expression in the integral floating system. Moreover, the appearance of borders from the lenslets of the lenslet array can also be eliminated. Adopting a concave lens instead of a convex lens for the floating scheme is more beneficial for displaying a long-distance 3D image. As conceptually depicted in Fig. 2, the concave floating lens images the lenslet array and the elemental image with a magnification factor

less than one, i.e., the lateral size is reduced; this is unlike the conventional integral floating system with a convex floating lens. The entire system can be interpreted as an InIm system composed of the effective lenslet array and elemental images that are images of the actual lenslet array and elemental images transformed by the concave floating lens. With a simple calculation, the effective parameters of the effective lenslet array and elemental image are

$$p_e = \frac{1}{G/F + g/F + 1} p,$$
$$\varphi_e = \frac{1}{G/F + 1} \varphi,$$
$$f_e = \frac{1}{(G/F + 1)^2} f. \tag{13}$$

This means that the effective InIm system is composed of an elemental image with a pixel pitch, which is the fundamental source of the 3D image quality, reduced by the factor of $(G/F + g/F + 1)$. As discussed in Section 2, the effective system is capable of displaying a more distant 3D image because the upper limit of the location of the central depth plane can be increased according to the ratio G/F. The effective InIm system can be designed to have a viewing angle parameter Ω and a lenslet pitch φ_o by adopting a lenslet array with the following parameters:

$$\varphi = (G/F + 1)\varphi_o,$$
$$f = (G/F + 1)^2$$
$$f_e \approx (G/F + 1)^2 \frac{\varphi_o}{\Omega}, \tag{14}$$

where the approximation holds for the sufficiently far location of the central depth plane. Hence, for the case where the integrated image is displayed at a far distance, the viewing angle of the lenslet array adopted for the system can be estimated as

$$\Omega_o \approx \frac{\varphi}{f} = \frac{1}{(G/F + 1)} \frac{\varphi_e}{f_e} \approx \frac{1}{(G/F + 1)} \Omega. \tag{15}$$

Equation (15) shows that the appropriate lenslet array for the system should have a much narrower viewing angle than the required value. The lenslet array that can be used for the system is generally useless by itself because of the narrow viewing angle. Hence, it is usually not commercially available and customization is needed. Nonetheless, the physical implementation of our system is guaranteed because the narrow viewing angle corresponds to a larger radius of curvature of each lenslet.

Figure 9 shows how much the proposed system can enhance the upper bound of the central depth plane according to the adopted concave lens. The pixel pitch of the display device is set to 0.1 mm for the simulation. The effective lenslet pitch and the viewing angle parameter Ω must be 2 mm and 0.33, respectively. L is the upper bound of the proposed system and L_o is the upper bound of the ordinary InIm system satisfying the same lenslet pitch and viewing angle. As G becomes larger, the upper bound of L is further extended because of the increased reduction factor of the pixel pitch of the display device. However, a larger G means that the adopted display device has a larger lateral size for displaying images of the same size. Hence, the ratio between G and F should be determined by considering the volume of the implemented system and the system becomes more efficient as F becomes smaller. However, the smaller F value usually causes lens distortion and severely affects the quality of the displayed image. Hence, the values of F and G should be carefully designed by considering various factors.

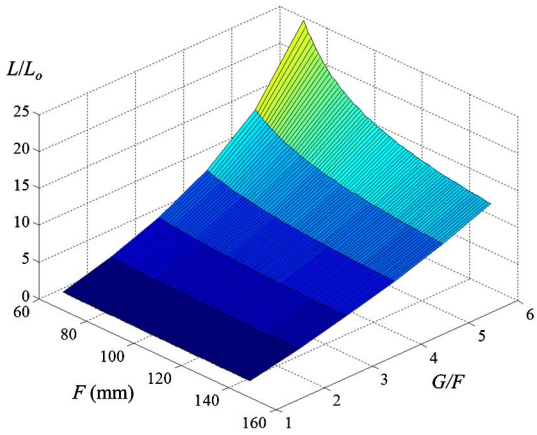

Fig. 9. (Color online) Simulation result showing the extended upper bound of L according to G and F.

The proposed integral floating system should have the ability to mix a real-world scene with a displayed 3D image in order to be used as an AR system. The easiest way to achieve such a mixture is to adopt a half mirror between the observer and the proposed system. However, an optical system adopting a half mirror always suffers from a large implementation volume, which makes it inadequate for HMD application. Instead of using the simple flat half mirror, the volume of the system can be reduced by applying the concept of a convex half mirror that combines the functions of a convex mirror and a half mirror. The concept of the convex half mirror, which is an optical component that functions as a convex mirror for the reflected light only, was proposed in our previous works [18,19]. Considering the implementation, the convex half mirror should have a structure whose external shape is a transparent plate with a thin convex half mirror embedded, as shown in Fig. 1, which depicts the concept of the HMD system based on the integral floating scheme implemented by a convex half mirror. Though a similar scheme was presented, the previous research focused on the implementation of an integral floating display with a convex lens [20].

A convex half-mirror fabrication process similar to the processes proposed in our previous research

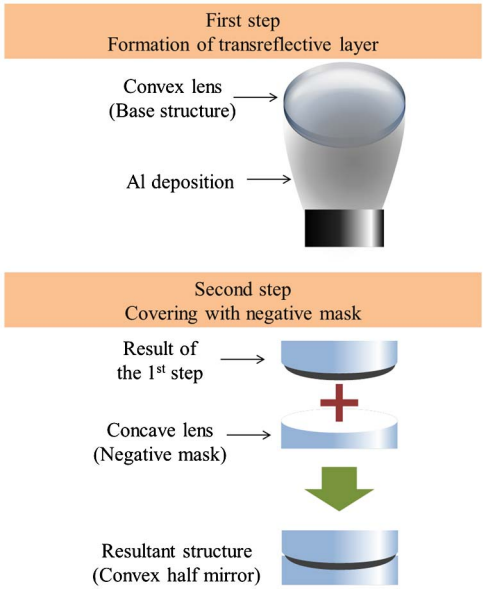

Fig. 10. (Color online) Fabrication process of convex half mirror.

[18,19] can be established. Actually, it is a simpler process because the target structure includes only one convex mirror, unlike the target of previous research involving an array of mirrors. Hence, the complicated index matching process presented in the previous research does not need to be incorporated. Figure 10 shows the fabrication process for implementing the convex half mirror prototype. It starts with the preparation of the convex lens for the base structure that will determine the shape of convex mirror in the completed convex half mirror. As the first step, a transreflective layer is formed on the prepared convex lens. A thin metallic layer formed by the deposition of Al is usually used for the transreflective layer. For the second step, the resultant structure of the first step is covered with a concave lens corresponding to the negative mask of the base structure. Though the pair of convex and concave lenses that can implement the prototype is easily available commercially, customization might be needed to obtain a certain specific convex mirror focal length.

4. Experimental Results

A preliminary experiment was performed to show the feasibility of our proposed scheme, which uses a concave lens for an integral floating system to display 3D images that are located a great distance from the observer. As we stated in the previous section, a lenslet array adequate for our scheme is generally not available as a readymade product because of an extremely small viewing angle. Instead, an experiment was performed with an ordinary lenslet array to prove the validity of our method for interpreting the proposed system as an effective InIm system. The system was configured as shown in Fig. 1. The detailed system specifications are listed in Table 1. Figure 11 shows a series of camera-captured

Table 1. System Specifications for the Experimental Setup of the Integral Floating Display Using a Concave Lens

Parameters	
Pixel pitch of display device, p	124.5 μm × 124.5 μm
Focal length of lenslet array, f	30 mm
Pitch of each lenslet, φ	5 mm × 5 mm
Focal length of concave lens, $-F$	−100 mm
Gap between lenslet array and concave lens, G	100 mm
Effective focal length of lenslet array, f_e	7.5 mm
Effective pitch of lenslet array, φ_e	2.5 mm × 2.5 mm

integrated images displayed by a proposed integral floating system with a concave lens. The considerably enhanced fundamental capability gained by the effectively reduced pixel pitch is used for enlarging the viewing angle because an ordinary lenslet array was adopted. As shown in Table 1, the upper bound of L calculated by Eq. (12) is around 40 mm. However, the range in which voxels exist extends to around 300 mm, according to Eq. (11). InIm images with L varying from 40 to 300 mm were

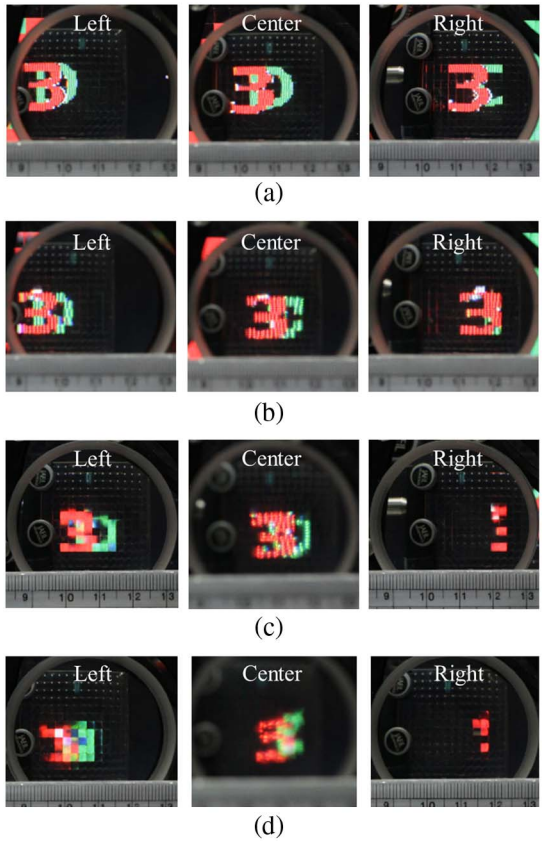

Fig. 11. (Color online) Camera-captured images showing the disparity in integrated images displayed by an integral floating system with a concave lens for various values of L: (a) $L = 40$ mm, (b) $L = 70$ mm, (c) $L = 149$ mm, (d) $L = 300$ mm. For each L, "3" and "D" are located 10 mm in front of and behind the central depth plane. For (c) and (d), the camera focus could not cover both the ruler and the integrated image. The center images of (c) and (d) are focused at integrated images.

Table 2. Comparison of Theoretical and Experimental Values of L and θ Using an Interpretation of the Proposed System as an Effective InIm System

Figure 11	Target L (mm)	Theoretical θ (°)	Measured L (mm)	Measured θ (°)
(a)	40	22.4	38	20.1
(b)	70	20.9	62	18.0
(c)	149	19.9	132	15.3
(d)	300	19.4	315	16.0

displayed. For comparison with the theoretical values, L and θ were experimentally calculated by measuring the disparity value with a ruler located in front of the concave lens. Table 2 presents the comparison results in which the experimentally obtained characteristic values are a good match to those of the effective InIm theoretical model system. Hence, we can conclude that the fundamental capability of the InIm scheme has been enhanced by our scheme. The series of camera-captured images, Fig. 11, show that the central depth plane located near the upper bound, 40 mm, provides acceptable integrated image visual quality. However, the visual quality degrades as the central depth plane grows farther from 40 mm. When $L = 300$ mm, the quality of the displayed integrated image is degraded to a level where the shape is not easily recognized, although the voxel still exists at that distance because the angular resolution of the displayed image reaches the limit determined by human visual acuity. The distortion of the lenslet of the lenslet array is another reason for the degraded image quality. Hence, the experimental results reveal the following: (1) the upper bound of L determined by Eq. (12) provides a good guideline for displaying an integrated image with an acceptable visual quality, (2) the interpretation of our proposed method, which considers the system to be an effective InIm system, explains well the investigated experimental results.

The adoption of a convex half mirror for HMD application was proposed in Section 3. A prototype convex half mirror (shown in Fig. 12) was implemented using the fabrication process shown in Fig. 10. The convex lens used for the prototype has a focal length of 100 mm and a pitch of 50 mm. The transreflective layer was formed by Al deposition and the thickness was controlled to make the reflectance

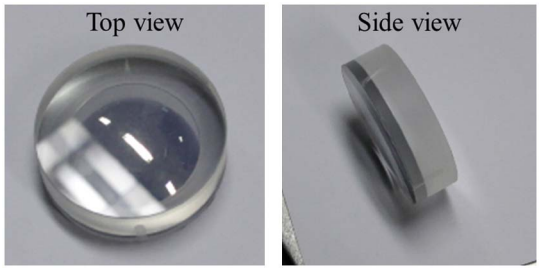

Fig. 12. (Color online) Implemented prototype of convex half mirror.

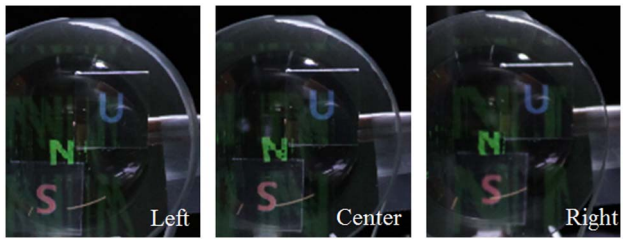

Fig. 13. (Color online) Camera-captured images of integrated image "N" displayed by the integral floating system adopting a convex half mirror. L was set to 30 mm. Real objects "S" and "U," which are printed on pieces of paper, were located for disparity comparison. "U" is located at the same distance as "N," while "S" is 30 mm behind "N" and "U."

50%. The focal length is shortened to about −25 mm when the optical concave lens function is provided by the transreflective convex mirror [21]. It is difficult to secure a sufficient optical path length when implementing the system because of the short focal length. Hence, a convex lens with a much larger focal length is required for the base structure when fabricating a convex half mirror for the actual product. The see-through characteristic of the convex half mirror and the feasibility of an integral floating scheme that adopts a convex half mirror instead of a concave lens are shown in experiments using our prototype. Figure 13 shows the camera-captured images of experimental results with the lenslet array and display device listed in Table 1. The real object that is located behind the convex half mirror is shown directly to the observer because of the see-through characteristic of the convex half mirror. The convex half mirror also displays the integrated image according to the principle of the integral floating system with a concave lens. A ghost artifact appears because of reflection at the convex half-mirror surface. It might be possible to avoid such artifacts by using an antireflective coating on the surface. The proposed system cannot implement real-world scene occlusions, like many other see-through displays. The real-world scene will dominate over the integrated image when the brightness of the real-world scene is significant compared to the integrated image. Hence, the brightness of the integrated image should be sufficiently high to suppress perception of the overlapped real world scene.

5. Conclusion

In this article, we have proposed a novel integral floating scheme that adopts a concave lens instead of a convex lens. As discussed, the proposed system can be interpreted as an effective InIm system in which all of the system specifications have been changed. The pixel pitch of the display panel is reduced and is helpful in extending the upper bound of the location of the central depth plane, as explained in the previous sections. However, a lenslet array with an extraordinarily small viewing angle should be adopted in order to obtain a meaningful viewing angle and lenslet pitch when it is

transformed to an effective InIm system. Such a lenslet array is usually not commercially available because, by itself, it is useless. Fortunately, a lenslet array with a smaller viewing angle is physically realizable. Hence, it is possible to customize the lenslet array for the intended specifications. We have also demonstrated that the optical see-through HMD, which is capable of displaying a 3D image with a proper accommodation cue, can be implemented by adopting a convex half mirror for our proposed integral floating scheme. Actually, the focal length of the convex lens prepared for the base structure of the convex half mirror must be sufficiently long to secure a sufficient optical path length. The feasibility of our proposed system was verified with a prototype implemented using the commercially available lenslet array, convex lens, and concave lens. An actual system capable of providing 3D images with a see-through property at far distances is expected to be implemented using the customized optical components.

This research was supported by the Ministry of Knowledge Economy (MKE), Korea, as part of a project called "Development of an Interactive User Interface Based 3D System."

References

1. F. Zhou, H. B.-L. Duh, and M. Billinghurst, "Trends in augmented reality tracking, interaction and display: a review of ten years of ISMAR," in *Proceedings of 7th IEEE/ACM International Symposium* (IEEE, 2008), pp. 193–202.
2. O. Cakmakci and J. Rolland, "Head-worn displays: a review," J. Disp. Technol. **2**, 199–216 (2006).
3. S. Liu, H. Hua, and D. Cheng, "A novel prototype for an optical see-through head-mounted display with addressable focus cues," IEEE Trans. Vis. Comput. Graph. **16**, 381–393 (2010).
4. Y. Takaki, Y. Urano, S. Kashiwada, H. Ando, and K. Nakamura, "Super multi-view windshield display for long-distance image information presentation," Opt. Express **19**, 704–716 (2011).
5. Y. Takaki and N. Nago, "Multi-projection of lenticular displays to construct a 256-view super multi-view display," Opt. Express **18**, 8824–8835 (2010).
6. J. Hong, Y. Kim, H.-J. Choi, J. Hahn, J.-H. Park, H. Kim, S.-W. Min, N. Chen, and B. Lee, "Three-dimensional display technologies of recent interest: principles, status, and issues," Appl. Opt. **50**, H87–H115 (2011).
7. Y. Kim, J. Kim, K. Hong, H. K. Yang, J.-H. Jung, H. Choi, S.-W. Min, J.-M. Seo, J.-M. Hwang, and B. Lee, "Accommodative response of integral imaging in near distance," J. Disp. Technol. **8**, 70–78 (2012).
8. F. Jin, J. Jang, and B. Javidi, "Effects of device resolution on three-dimensional integral imaging," Opt. Lett. **29**, 1345–1347 (2004).
9. J.-H. Park, S.-W. Min, S. Jung, and B. Lee, "Analysis of viewing parameters for two display methods based on integral photography," Appl. Opt. **40**, 5217–5232 (2001).
10. S.-W. Min, J. Kim, and B. Lee, "New characteristic equation of three-dimensional integral imaging system and its applications," Jpn. J. Appl. Phys. **44**, L71–L74 (2005).
11. J.-H. Park, K. Hong, and B. Lee, "Recent progress in three-dimensional information processing based on integral imaging," Appl. Opt. **48**, H77–H94 (2009).
12. G. Park, J.-H. Jung, K. Hong, Y. Kim, Y.-H. Kim, S.-W. Min, and B. Lee, "Multi-viewer tracking integral imaging system and its viewing zone analysis," Opt. Express **17**, 17895–17908 (2009).
13. F. W. Campbell and D. G. Green, "Optical and retinal factors affecting visual resolution," J. Physiol. **181**, 576–593 (1965).
14. K. Hong, J. Hong, J.-H. Jung, J.-H. Park, and B. Lee, "Rectification of elemental image set and extraction of lens lattice by projective image transformation in integral imaging," Opt. Express **18**, 12002–12016 (2010).
15. T. Nagoya, T. Kozakai, T. Suzuki, M. Furuya, and K. Iwase, "The D-ILA device for the world's highest definition (8K4K) projection systems," in *Proceedings of International Display Workshop* (Society for Information Display, 2008), pp. 203–206.
16. J. Kim, S.-W. Min, Y. Kim, and B. Lee, "Analysis on viewing characteristics of integral floating system," Appl. Opt. **47**, D80–D86 (2008).
17. J. Kim, S.-W. Min, and B. Lee, "Viewing region maximization of an integral floating display through location adjustment of viewing window," Opt. Express **15**, 13023–13034 (2007).
18. J. Hong, Y. Kim, S.-G. Park, J.-H. Hong, S.-W. Min, S.-D. Lee, and B. Lee, "3D/2D convertible projection-type integral imaging using concave half mirror array," Opt. Express **18**, 20628–20637 (2010).
19. J. Hong, J. Kim, and B. Lee, "Two-dimensional/three-dimensional convertible integral imaging using dual depth configuration," Appl. Phys. Express **5**, 012501 (2012).
20. J. Jung, J. Hong, B. Lee, and S.-W. Min, "Augmented reality system based on integral floating method," in *Digital Holography and Three-Dimensional Imaging*, OSA Technical Digest (CD) (Optical Society of America, 2011), paper DTuC22.
21. Y. Kim, S.-G. Park, S.-W. Min, and B. Lee, "Integral imaging system using a dual-mode technique," Appl. Opt. **48**, H71–H76 (2009).